

Discrete-time picture for multiphoton microwave spectroscopy

M. J. Cavagnero and S. T. Cornett*

Department of Physics and Astronomy, University of Kentucky, Lexington, Kentucky 40506-0055

(Received 27 November 1996)

The time evolution of atomic and molecular systems driven by periodic external fields is reformulated to combine Floquet's theorem with time-dependent representations of the atomic degrees of freedom. This approach increases the flexibility of Floquet calculations of multiphoton processes in strong radiation fields, particularly at low frequencies, by incorporating adiabatic states into the basis. The depopulation of Rydberg states of He and Na in strong microwave fields illustrates the utility of the method. In particular, a study of the depopulation of the $11s$ state of Na in an oscillatory field reveals a strong correspondence between dc-field Stark maps and quasienergy spectra and predicts a resonance feature associated with Landau-Zener transitions between dc Stark levels. [S1050-2947(97)02605-X]

PACS number(s): 32.80.Rm, 31.15.-p

I. INTRODUCTION

Theoretical studies of atoms subjected to intense electromagnetic fields frequently focus on the calculation of quasienergy spectra that characterize the quasiperiodic modes of an atom-field system. Such studies, referred to here as Floquet spectroscopy, date from Shirley's application [1] of Floquet's theorem [2] to the time evolution of a two-level atom in a strong, oscillatory electric field [3]. Floquet spectroscopy serves now widely to interpret multiphoton processes including the excitation and ionization of atoms and the dissociation of molecules [4]. The method has recently been extended to calculate inelastic ion-atom collision cross sections [5]. Shirley's method hinges on truncating and diagonalizing a sparse, infinite Hamiltonian matrix $\langle N', n' | H_F | N, n \rangle$ indexed by the atomic state (N) and a Fourier component (n) of the state amplitude. Eigenvectors of this matrix represent quasistationary states that, when superimposed to match initial conditions, determine the system's time evolution matrix.

This paper demonstrates how a unitary transformation of Shirley's truncated Hamiltonian matrix affords using time-dependent basis functions, such as adiabatic functions, to represent atomic degrees of freedom. This result greatly increases the flexibility of Floquet calculations, usually confined to an atomic-state representation, by tailoring basis sets to different regimes of time or field strength. This approach closely relates to the discrete-variable representations of Schrödinger's equation used by Light and others [6–8] in calculating molecular processes on a grid of space and/or time points. The utility of our approach to Floquet spectroscopy is illustrated here through applications to the microwave depopulation of prepared Rydberg states of He and Na [9].

Section II summarizes Shirley's formulation of the Floquet Hamiltonian. Section III presents the unitary transformation to a discrete-time variable and Sec. IV provides an

explicit form of the Floquet Hamiltonian in the adiabatic representation. In the absence of dc fields, the Floquet Hamiltonian is invariant [10] under the product PT of parity P and time translation by one half of the period of the driving field $\mathcal{T}f(t) = f(t + \pi/\omega)$. This exact symmetry is exploited in Sec. V to reduce the discrete-time lattice to a one-fourth cycle of the driving field. Applications to the multiphoton microwave spectroscopy of He and Na in Sec. VI are followed by concluding remarks in Sec. VII.

II. SHIRLEY'S FLOQUET HAMILTONIAN

Consider an atom with Hamiltonian H_a that is subjected to an externally applied field with frequency $\omega = 2\pi/T$. The atomic response to the external field is determined by Schrödinger's equation (in atomic units)

$$i \frac{\partial}{\partial t} |\Psi(t)\rangle = [H_a + H' \cos(\omega t)] |\Psi(t)\rangle, \quad (1)$$

where H' is typically a dipole transition operator.

Floquet's theorem stipulates that this equation has quasiperiodic solutions of the form

$$|\Psi(t)\rangle = e^{-i\gamma t} |\psi_\gamma(t)\rangle, \quad (2)$$

where $|\psi_\gamma(t)\rangle$ is periodic with period T ,

$$|\psi_\gamma(t + mT)\rangle = |\psi_\gamma(t)\rangle, \quad m = 0, \pm 1, \pm 2, \pm 3, \dots \quad (3)$$

Equations (1) and (2) imply the eigenvalue equation for the quasienergy γ ,

$$\gamma |\psi_\gamma(t)\rangle = \left[H_a + H' \cos(\omega t) - i \frac{\partial}{\partial t} \right] |\psi_\gamma(t)\rangle. \quad (4)$$

Equation (4) is cast in matrix form by expanding the periodic functions $|\psi_\gamma(t)\rangle$ in a Fourier series

$$|\psi_\gamma(t)\rangle = \sum_{n=-\infty}^{\infty} e^{in\omega t} |n\rangle |\psi_\gamma\rangle \quad (5)$$

whose amplitudes satisfy the recurrence relations

*Present address: Institute for Theoretical Atomic and Molecular Physics, Harvard-Smithsonian Center for Astrophysics, Harvard University, 60 Garden Street, Cambridge, MA 02138.

$$\begin{aligned} \gamma(n|\psi_\gamma) &= (H_a + n\omega)(n|\psi_\gamma) + \frac{1}{2}H'[(n+1|\psi_\gamma) \\ &+ (n-1|\psi_\gamma)]. \end{aligned} \quad (6)$$

The coordinate dependence of $(n|\psi_\gamma)$ is typically represented by an expansion in orthonormal eigenstates of the atomic Hamiltonian,

$$(n|\psi_\gamma) = \sum_N |N\rangle\langle Nn|\psi_\gamma\rangle, \quad (7)$$

whose sum extends over the continuous spectrum. Equation (6) is then written in the atomic state representation as

$$\begin{aligned} \gamma\langle Nn|\psi_\gamma\rangle &= \sum_{m,M} \left[(E_N + n\omega)\delta_{N,M}\delta_{n,m} + \frac{1}{2}\langle N|H'|M\rangle \right. \\ &\left. \times (\delta_{m,n+1} + \delta_{m,n-1}) \right] (Mm|\psi_\gamma), \end{aligned} \quad (8)$$

Shirley's infinite-dimensional, discrete eigensystem [1]. The matrix in angular brackets is generally referred to as the Floquet Hamiltonian, $\langle N,n|H_F|M,m\rangle$.

Most practical applications of Shirley's method conveniently restrict the sum in Eq. (7) to a finite number of atomic states, considering only transitions among them. This inessential restriction to a finite vector space will be retained here for simplicity. Only transitions among a set of N_0 atomic levels, designated $N=1,2,\dots,N_0$, are considered here.

The eigenvalues of Eq. (8) are periodic [1], taking the form

$$\gamma = \sigma + s\omega, \quad s=0,\pm 1,\pm 2,\pm 3,\dots, \quad (9)$$

with N_0 values of σ in the range

$$-\omega/2 \leq \sigma \leq \omega/2. \quad (10)$$

The eigenvectors corresponding to the quasienergies in this range [i.e., with $s=0$ in Eq. (9)] yield a set of N_0 independent solutions of the time-dependent Schrödinger equation whose superposition satisfies an arbitrary initial condition. Accordingly, while the dimension of the Floquet Hamiltonian is infinite, we utilize only N_0 quasienergies in the range Eq. (10) and their corresponding eigenvectors to construct the time-evolution matrix.

Numerical solution of the infinite-dimensional system Eq. (8) proceeds by truncating the harmonic expansion Eq. (5) to a range of $2K+1$ values

$$|\psi_\gamma^K(t)\rangle = \sum_{n=-K}^K e^{in\omega t} (n|\psi_\gamma^K). \quad (11)$$

The eigensystem Eq. (8) is then of finite linear dimension $[N_0(2K+1)]$ and efficient algorithms are available for determining the selected eigenvalues and eigenvectors of the sparse system. The number of harmonics required for convergence of this expansion is determined numerically by

testing the periodicity of the quasienergy spectrum's center or the convergence of the corresponding transition probability [11].

From the eigenvectors of Eq. (8), which we denote by $\langle N,n|\psi_{\sigma,s}\rangle$ in accordance with Eq. (9), Shirley [1] constructed the evolution matrix

$$\begin{aligned} U_{MN}(t,t_0) &= \sum_n \sum_{\sigma,s} e^{in\omega t} \langle M,n|\psi_{\sigma,s}\rangle e^{-i(\sigma+s\omega)(t-t_0)} \\ &\times \langle \psi_{\sigma,s}|N,0\rangle \end{aligned} \quad (12)$$

and the corresponding transition probability

$$P_{N\rightarrow M}(t,t_0) = |U_{MN}(t,t_0)|^2. \quad (13)$$

This equation is now averaged over t_0 holding the elapsed time $t-t_0$ fixed since t_0 is determined by a random process, such as the entry of the atom into the radiation field (or microwave cavity). Averaging the result over the elapsed time as well, Shirley arrived at the infinite-cycle-averaged transition probability

$$\bar{P}_{N\rightarrow M} = \sum_\sigma T_{M\sigma} T_{N\sigma}, \quad (14)$$

with

$$T_{N,\sigma} = \sum_n |\langle N,n|\psi_{\sigma,0}\rangle|^2. \quad (15)$$

While Eq. (14) is only appropriate [1] when details of the microwave field's envelope are irrelevant, it nevertheless provides useful comparisons of alternative calculations and serves to analyze our results in Sec. VI.

As an introduction to Sec. V on PT invariance, we note here that if atomic states N and M have the same (opposite) parity, then only even (odd) values of n contribute to the sum in Eq. (12). The Floquet Hamiltonian is accordingly block diagonal in PT . The periodic parts $|\psi_{\sigma,s}(t)\rangle$ of the Floquet solutions are PT eigenstates with eigenvalue $(-1)^{q(\sigma,s)}$. The corresponding eigenvectors $\langle N,n|\psi_{\sigma,s}\rangle$ vanish unless $(-1)^{P(N)+n} = (-1)^{q(\sigma,s)}$. [Note that the full Floquet solutions are not even or odd under PT , due to the phase factor in Eq. (2).]

It may at first appear surprising that the evolution matrix in Eq. (12) is constructed solely from PT eigenstates with eigenvalue $(-1)^{P(N)}$, where N is the initial atomic state. However, from the symmetry of the Floquet eigenvectors, it follows that for each Floquet state with an even- PT periodic part, there is an identical Floquet state with an odd- PT periodic part whose quasienergy is shifted by one unit of the driving frequency. Accordingly, only even (or odd) PT eigenstates are required in constructing the evolution matrix.

III. THE DISCRETE-TIME TRANSFORMATION

The Fourier expansion of the Floquet states in Eq. (11) appears to require basis states that are independent of time, as in the atomic state expansion Eq. (7). However, Floquet's theorem does not require the use of a Fourier series; it only proves the existence of a set of quasiperiodic solutions sat-

isfying Eqs. (2) and (3). In principle, the periodic part of a Floquet solution can be represented by *any complete set of periodic functions*; any unitary transformation of the $2K+1$ harmonics $\exp(in\omega t)$ will yield an equivalent representation of the dynamics to the extent that a truncated expansion [as in Eq. (11)] converges.

An alternative set of periodic harmonics for expanding the Floquet solutions is constructed here by diagonalizing the time dependence of the interaction, that is, by diagonalizing the matrix

$$\begin{aligned} (m|\cos\omega t|n) &\equiv \frac{1}{T} \int_0^T dt e^{-im\omega t} \cos(\omega t) e^{in\omega t} \\ &= \frac{1}{2} [\delta_{m,n+1} + \delta_{m,n-1}], \quad |m| \leq K, \quad |n| \leq K. \end{aligned} \quad (16)$$

This diagonalization, familiar from the classical analysis of the vibration of a string fixed at its end points [12], yields eigenvalues

$$\cos\left(\frac{\tau\pi}{2K+2}\right), \quad \tau = 1, 2, 3, \dots, 2K+1, \quad (17)$$

corresponding to eigenvectors

$$(n|\tau) = \frac{1}{\sqrt{K+1}} \sin\left(\frac{n\tau\pi}{2K+2} + \frac{\tau\pi}{2}\right), \quad -K \leq n \leq K. \quad (18)$$

The resultant harmonic functions of time

$$\begin{aligned} (t|\tau) &= \sum_{n=-K}^K e^{in\omega t} (n|\tau) \\ &= e^{i\pi(\tau-1)t/2} \frac{\sin\left(\frac{\tau\pi}{2K+2}\right)}{\sqrt{K+1}} \frac{\sin[(K+1)\omega t + \tau\pi/2]}{\left[\cos(\omega t) - \cos\left(\frac{\tau\pi}{2K+2}\right)\right]}, \end{aligned} \quad (19)$$

are orthonormal, satisfying

$$(\tau'|\tau) = \sum_{m=-K}^K (\tau'|m)(m|\tau) = \frac{1}{T} \int_0^T dt (\tau'|t)(t|\tau) = \delta_{\tau',\tau}, \quad (20)$$

with eigenvalue $(-1)^{\tau+1}$ (even or odd) under time reversal $t \rightarrow -t$.

The harmonic functions defined by Eq. (19) are periodic in time, related to the exponential harmonics by the unitary transformation Eq. (18). Figure 1 displays a few of these harmonics, plotted versus t/T , for the particular case $K=10$. Note how each harmonic is strongly peaked in the vicinity of its eigenvalue $t/T = \tau/2(2K+2)$ and is similar in appearance to a diffraction pattern; they are referred to as ‘‘diffractive harmonics’’ from this point forward. Similar harmonic functions occur in discrete-variable representations of Schrödinger’s equation [8].

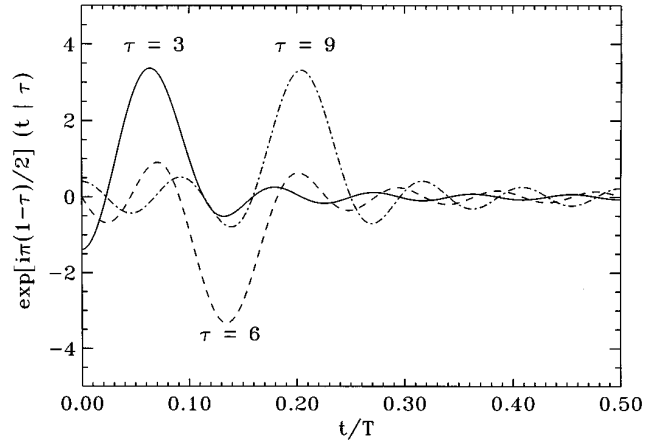


FIG. 1. Diffractive harmonics used in the discrete-time representation, with $K=10$ and $\tau=3, 6,$ and 9 , respectively.

We now replace the Fourier series Eq. (11) by its alternative expansion in diffractive harmonics

$$|\psi_\gamma^K(t)\rangle = \sum_{\tau=1}^{2K+1} (t|\tau)(\tau|\psi_\gamma^K). \quad (21)$$

Substituting this expansion into Eq. (4) and using the orthogonality relation Eq. (20) yields the recurrence relations

$$\begin{aligned} \gamma(\tau|\psi_\gamma^K) &= \left[H_a + H' \cos\left(\frac{\tau\pi}{2K+2}\right) \right] (\tau|\psi_\gamma^K) \\ &\quad + \sum_{\tau'} \Lambda_{\tau,\tau'} (\tau'|\psi_\gamma^K), \end{aligned} \quad (22)$$

with the matrix element between discrete times τ and τ' ,

$$\begin{aligned} \Lambda_{\tau,\tau'} &= \left(\tau \left| \frac{1}{i} \frac{\partial}{\partial t} \right| \tau' \right) \\ &= \begin{cases} 0, & \text{for } \tau + \tau' \text{ even} \\ \frac{\omega}{K+1} \frac{\sin\left(\frac{\tau\pi}{2K+2}\right) \sin\left(\frac{\tau'\pi}{2K+2}\right)}{\left[\cos\left(\frac{\tau'\pi}{2K+2}\right) - \cos\left(\frac{\tau\pi}{2K+2}\right)\right]^2} \end{cases} \end{aligned} \quad (23)$$

for $\tau + \tau'$ odd.

The phase factor in Eq. (19) ensures that the derivative matrix is real and symmetric to make the last term in Eq. (22) Hermitian. The derivative matrix is strongly peaked about $\tau = \tau' \pm 1$. Equation (22) reduces directly to Eq. (4) in the limit $K \rightarrow \infty$.

The recurrence relations Eq. (22) are equivalent to Eq. (6) provided the truncation to $2K+1$ harmonics converges. Equation (22) amounts primarily to a simple ‘‘discretized’’ form of Schrödinger’s equation over a half cycle of the driving field, an aspect apparently overlooked in the past. It will serve to reduce the vector space of atomic states to those few adiabatic states relevant to specific transition processes.

IV. THE ADIABATIC REPRESENTATION

The expansion in atomic eigenstates $|N\rangle$, used in Eq. (7) and common to most applications of Shirley's method, may now be replaced by an expansion in adiabatic states, defined at discrete times τ as solutions of the eigenvalue equation

$$\left[H_a + H' \cos\left(\frac{\tau\pi}{2K+2}\right) \right] |\mu; \tau\rangle = \epsilon_\mu(\tau) |\mu; \tau\rangle. \quad (24)$$

The coordinate dependence of the eigenvector $(\tau|\psi_\gamma^K\rangle)$ of Eq. (22) is then expanded into eigenvectors of Eq. (24),

$$(\tau|\psi_\gamma^K\rangle) = \sum_\mu |\mu; \tau\rangle \langle \mu; \tau | \psi_\gamma^K \rangle. \quad (25)$$

Substitution of this expansion into Eq. (22) and use of the orthonormality of the adiabatic states for fixed τ yields the eigensystem

$$\gamma(\mu; \tau | \psi_\gamma^K) = \sum_{\mu', \tau'} \langle \mu; \tau | H_F | \mu'; \tau' \rangle \langle \mu'; \tau' | \psi_\gamma^K \rangle, \quad (26)$$

where

$$\langle \mu; \tau | H_F | \mu'; \tau' \rangle = \epsilon_\mu(\tau) \delta_{\mu, \mu'} \delta_{\tau, \tau'} + \Lambda_{\tau, \tau'}(\mu; \tau | \mu'; \tau'). \quad (27)$$

This result replaces the original Shirley form of the Floquet Hamiltonian. This discrete-time representation of the truncated Floquet Hamiltonian requires adiabatic eigenvalues at $2K+1$ discrete times, and an overlap matrix of adiabatic states at different discrete times. Here, as in many physical applications, the time evolution of the system remains largely confined to adiabatic or near-adiabatic pathways. Our form of the Floquet Hamiltonian affords truncating the matrix to the adiabatic pathways of interest, as demonstrated in Sec. VI.

V. PT INVARIANCE

In the absence of dc fields, the atomic Hamiltonian H_a commutes with the parity operator P . As a result, the Floquet Hamiltonian operator in Eq. (4) commutes with PT , where T shifts t by a half-period $\mathcal{T}f(t) = f(t + \pi/\omega)$. This symmetry has served previously to reduce the dimension of the Floquet matrix [10]. In this section, we apply this symmetry to the Floquet matrix in the discrete-time picture.

Eigenstates of PT ,

$$P\mathcal{T}|\mu, q; \tau\rangle = (-1)^q |\mu, q; \tau\rangle, \quad (28)$$

are readily constructed by expansion into products of adiabatic states and diffractive harmonics. Such products are denoted here by

$$|\mu, \tau\rangle = |\mu; \tau\rangle |\tau\rangle, \quad (29)$$

with the required transformation properties

$$T|\tau\rangle = (-1)^K |2K+2-\tau\rangle \quad (30)$$

and

$$P|\mu; \tau\rangle = |\mu; 2K+2-\tau\rangle \langle \mu; 2K+2-\tau | P | \mu; \tau \rangle. \quad (31)$$

These equations yield PT eigenstates in the form

$$|\mu, q; \tau\rangle = \frac{1}{\sqrt{2}} [|\mu, \tau\rangle + (-1)^{K+q} |\mu, 2K+2-\tau\rangle] \times \langle \mu; 2K+2-\tau | P | \mu; \tau \rangle, \quad (32)$$

for $\tau = 1, 2, \dots, K$, and

$$|\mu, q; K+1\rangle = |N_\mu, K+1\rangle, \quad (-1)^{P(N_\mu)} = (-1)^{q+K}, \quad (33)$$

where N_μ labels the atomic state of parity $P(N_\mu)$ (even or odd) coinciding with adiabatic state μ at zero field. Note that at the discrete time $\tau = K+1$ the adiabatic Hamiltonian reduces to H_a , so that Eq. (33) is a simple product of atomic state $|N_\mu\rangle$ and of the diffractive harmonic $|K+1\rangle$.

When transformed according to Eqs. (32) and (33), the Floquet Hamiltonian in Eq. (27) is diagonal in q . For $\tau \neq K+1$ and $\tau' \neq K+1$, the matrix elements are

$$\begin{aligned} \langle \mu, q; \tau | H_F | \mu', q; \tau' \rangle &= \epsilon_\mu(\tau) \delta_{\mu, \mu'} \delta_{\tau, \tau'} + \Lambda_{\tau, \tau'} \langle \mu; \tau | \mu'; \tau' \rangle \\ &\quad + (-1)^{K+q} \Lambda_{\tau, 2K+2-\tau'} \\ &\quad \times \langle \mu; \tau | P | \mu'; \tau' \rangle. \end{aligned} \quad (34)$$

For $\tau = K+1$ and $\tau' \neq K+1$, one finds

$$\begin{aligned} \langle \mu, q; K+1 | H_F | \mu', q; \tau' \rangle &= \frac{1}{\sqrt{2}} [1 + (-1)^{K+q+P(N_\mu)}] \Lambda_{K+1, \tau'} \langle N_\mu | \mu'; \tau' \rangle, \end{aligned} \quad (35)$$

and finally, for $\tau = \tau' = K+1$

$$\langle \mu; K+1 | H_F | \mu'; K+1 \rangle = \epsilon_\mu(K+1) \delta_{\mu, \mu'}. \quad (36)$$

The new Floquet Hamiltonian given by Eqs. (34)–(36) is real and symmetric and has half the linear dimension of the earlier result Eq. (27). Only the discrete-time points $\tau = 1, 2, \dots, K+1$ now enter the matrix, so that Floquet's theorem combined with PT symmetry results in discretizing Schrödinger's equation over a one-fourth cycle of the driving field. The eigenvalues of the Floquet Hamiltonian are now periodic with period 2ω [10] and only eigenvectors lying within $\pm\omega$ of the eigenvalue spectrum's center are needed to construct the evolution matrix.

Finally, we note that the infinite-cycle-averaged transition probability in Eq. (14) is invariant under our unitary tranfor-

mation to a discrete-time picture. The amplitudes in Eq. (15) are expressed in terms of the eigenvectors in this picture by

$$T_{N,\sigma} = \sum_{\tau=1}^{K+1} \sum_{\mu} \sum_{\mu'} \langle \sigma, 0 | \mu', q; \tau \rangle \langle \mu'; \tau | N \rangle \langle N | \mu; \tau \rangle \times \langle \mu, q; \tau | \sigma, 0 \rangle. \quad (37)$$

Note that, as with Shirley's derivation of Eq. (14), only even (or odd) PT eigenstates are required for the construction of the evolution matrix.

VI. APPLICATIONS

This section applies the method described above to the multiphoton, microwave spectroscopy of Rydberg atoms. H_a now represents the effective Hamiltonian of an atom consisting of a single, active electron orbiting an inert ionic core. H' is the product of the electric-field amplitude F and the dipole operator z . The adiabatic states $|\mu; \tau\rangle$ in Eq. (24) are Stark states evaluated at the field $F \cos(\tau\pi/2K+2)$; their evaluation has been described in detail previously [13].

Strong-field microwave studies of Rydberg atoms have focused primarily on atomic H, He, K, and Na [9]. In non-hydrogenic atoms, resonant multiphoton processes have been observed for field amplitudes comparable to the dc field amplitudes that mix adjacent n manifolds on a Stark map $F \sim 1/3n^5$. Interpretation of these multiphoton transitions in the case of He, for fields $F < 1/3n^5$, was facilitated by quasienergy spectra calculated by van de Water *et al.* [11] using Shirley's form of the Floquet Hamiltonian. That work demonstrated how Shirley's Hamiltonian can be truncated to a restricted basis of atomic states, provided enough zero-field states are included to reproduce the dc-field Stark map accurately. At higher fields, the large number of zero-field states required to produce an accurate Stark map prevents practical applications of Shirley's method.

Here we illustrate our discrete-time approach to multiphoton transitions by first reproducing the weak-field results of van de Water *et al.* in triplet He. We then analyze the microwave spectrum of Na in the n -mixing regime, finding features of the quasienergy spectrum attributable to specific avoided crossings on the dc-field Stark map.

A. Helium

The microwave depopulation and ionization of $n^3S(m_l=0)$ states of He were studied in Refs. [11,14]. We present below the results of alternative calculations of the quasienergy spectrum using (i) the standard Shirley form of the Floquet Hamiltonian Eq. (8) and (ii) the discrete-time Floquet Hamiltonian described above. Both calculations make use of PT symmetry, yielding periodic quasienergy spectra with period 2ω .

We focus on the survival probability of an initial $n=28^3S$ state. van de Water *et al.* have carefully accounted in their calculations for the shape of the microwave field envelope. Since we are concerned primarily with comparing the discrete-time method with a straightforward diagonalization of Shirley's Hamiltonian, we will ignore effects associated with the rise and fall of the microwave amplitude and simply calculate the infinite-cycle-averaged transition prob-

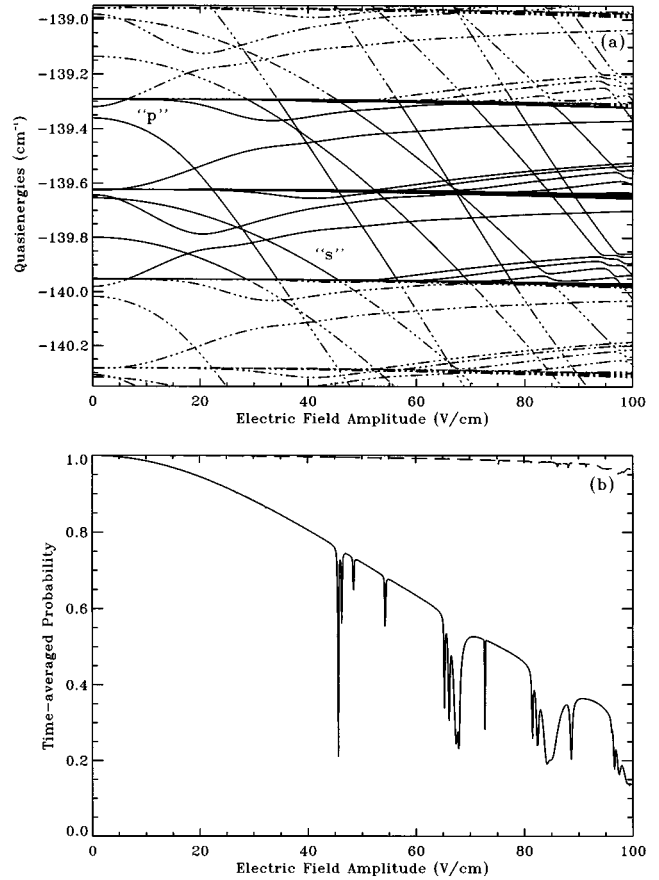


FIG. 2. (a) Quasienergies versus field amplitude for triplet-He atoms in a 9.924-GHz microwave field. Results were obtained in the discrete-time picture with 30 adiabatic basis states. The solid lines show the center spectrum of even PT states. The spectrum is periodic with period 2ω . The lines labeled s and p connect at zero field to the 28^3S and 29^3P states, respectively. (b) Survival probability of the 28^3S state as a function of field amplitude. The dashed line is the degree of unitarity of the calculation.

abilities obtained from Eqs. (14) and (37).

Our quasienergy spectrum for this system is shown in Fig. 2(a). The microwave frequency is 9.924 GHz, or 0.331 cm^{-1} . A set of adiabatic basis states was first constructed using 140 zero field states spanning the range of principal quantum numbers $26 \leq n \leq 30$; this range yields a Stark map that is accurate for fields up to at least 100 V/cm. (A reduced mass was used for the Rydberg electron, and quantum defects were taken from [14].) Thirty of these adiabatic states were then used for the construction of the Floquet matrix in the discrete-time picture. These adiabatic levels correspond at zero field to all states of the $n=28$ manifold plus the $n=29$, $l=0$, and $l=1$ states. These last two states were necessary to obtain a converged Floquet spectrum for microwave field amplitudes larger than 80 V/cm, which corresponds roughly to the fields at which $n=28$ and $n=29$ Stark states overlap. Eighty-one diffractive harmonics (corresponding to $K=40$) were necessary to obtain a periodic center spectrum. In our calculations, the 28^3S state at zero field was assumed to be the initial state. This state has a negative ac Stark shift for finite fields and is labeled "s" in the figure.

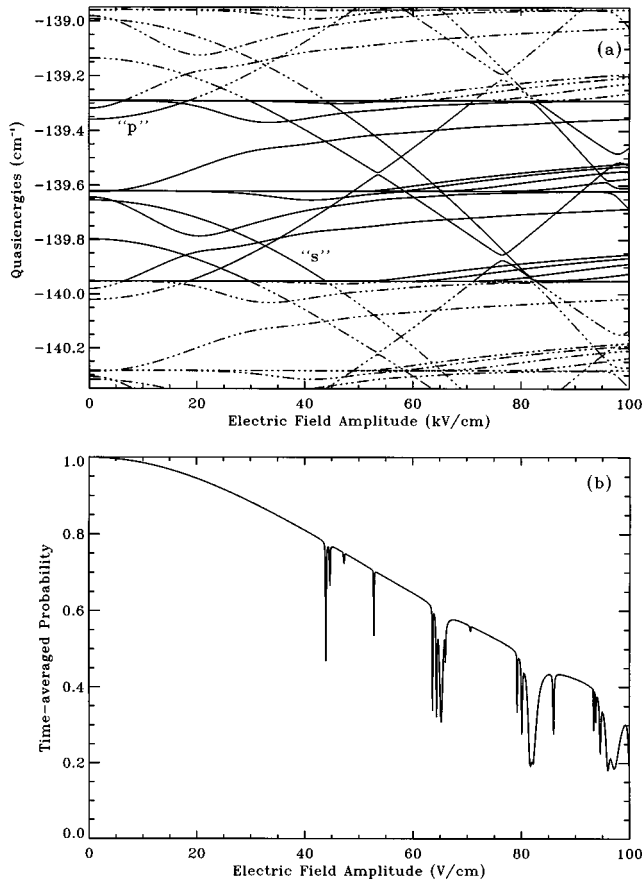


FIG. 3. Same as in Fig. 2, but calculated using Shirley's form of the Floquet Hamiltonian with 30 zero-field basis states. The dimension of the Floquet matrix is equal to that in Fig. 2. (a) Quasienergy spectrum. Note the positive ac Stark shift of the p state. (b) Survival probability of the 28^3S state.

The time-averaged survival probability of the 28^3S state is shown in Fig. 2(b). It displays a number of sharp resonant features in the intermediate field region dominated by intra-manifold transitions. (The widths of these resonances are determined by the size of the corresponding avoided crossings in the quasienergy spectrum [1].) These features correspond quite closely to those calculated in [11], where the standard Shirley form of the Floquet matrix was used and where transition probabilities were obtained taking into account the time variation of the field amplitude.

To facilitate comparison, we show in Fig. 3 the quasienergy spectrum and survival probability calculated using the standard form of the Floquet matrix. Again, 30 zero-field states were used as a basis. Note that the peaks in the discrete-time calculation Fig. 2(b) are noticeably shifted toward higher fields by a few V/cm in comparison to the peaks in Fig. 3(b). This shift results from the fact that an adiabatic basis yields more accurate ac Stark shifts than the zero-field basis. This shift has not yet been confirmed experimentally since the positions of the peaks were used in [11] to calibrate the microwave field amplitudes.

Another prominent difference between the two Floquet maps results from an incorrect ac Stark shift of the 29^3P state in the Shirley calculation [Fig. 3(a)]. A correct ac Stark shift of this state requires adding additional $n=29$ levels to

the basis. In contrast, the discrete-time picture does give a downward ac Stark shift for this state because of the natural curvature of the 29^3P adiabatic level.

It should also be noted that the discrete-time picture results in a small spreading (seen as dark bands) of the nearly degenerate manifold states in the quasienergy spectrum [Fig. 2(a)]. This spreading becomes appreciable for amplitudes greater than 80 V/cm, where significant differences between the two survival probability calculations can be seen. We will illustrate below the severe breakdown of the Shirley picture at these large fields for the case of atomic Na.

Also shown in Fig. 2(b) is the departure of our discrete-time calculations from unitarity. For our He calculations, unitarity is satisfied to within 5% over the range of fields studied. This lack of unitarity does not stem from an inadequate number of harmonics; the center of the quasienergy spectrum is quite periodic. The discrete-time approach is inherently nonunitary once the basis of adiabatic states is truncated. This results from the overlap matrix in the discrete-time Hamiltonian Eq. (27); that is, an adiabatic state at discrete-time τ will project onto an infinity of adiabatic states at time τ' . By truncating the matrix, we are neglecting transition amplitudes to other adiabatic levels. This departure from unitarity serves as a useful index of the degree of convergence of the adiabatic expansion. (We note that the exact unitarity of Shirley's method is artificial since states omitted from the basis are simply excluded from the vector space.)

In the low-field regime (0–80 V/cm), the He Stark states exhibit essentially diabatic behavior. It is not surprising that our calculation using adiabatic states gives results quite similar to those using a zero-field basis. Only when the field amplitude approaches the avoided crossing region on the dc Stark map are many zero-field states required for convergence, and, as discussed below, this region is where the discrete-time approach is most useful.

B. Sodium

When the microwave field amplitude is sufficient to drive intermanifold transitions, the standard approach to Floquet analysis becomes intractable. Even at zero frequency, constructing an accurate dc Stark map at these intermediate-field strengths requires a basis of several Rydberg manifolds. Transitions among the Rydberg manifolds in a slowly varying field require an accurate description of the avoided-crossing structures in the dc Stark map [15]. With more zero-field states required in the basis, a larger number of photons are also needed to bridge the increasing energy gap among the most distant states. Accordingly, the dimension of the Floquet Hamiltonian increases rapidly.

Furthermore, it is known experimentally that ionization of the atom becomes important at these intermediate fields [9]. One of the primary purposes of this investigation was to study the $n \rightarrow n+1$ transitions that are regarded as the rate-limiting step of microwave ionization of alkali-metal atoms and to show that this process can be described using a relatively simple Floquet calculation.

For this purpose, we have performed Floquet calculations for the depopulation of the $11s$ state of atomic Na. Our choice of Na is motivated primarily by the large avoided crossing between the $11s$ state and the lowest member of the

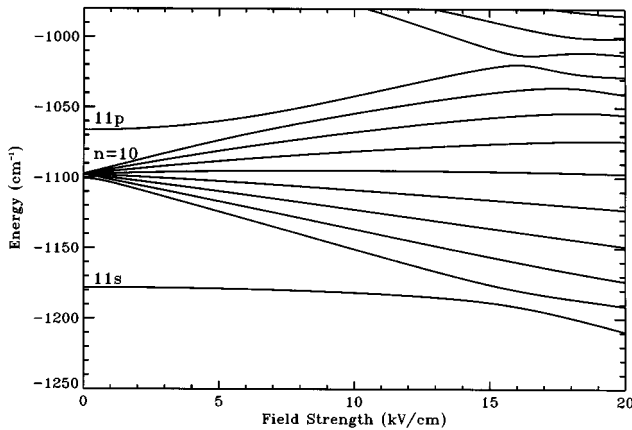


FIG. 4. Na adiabatic Stark map ($m=0$) in the energy region near the $n=10$ Rydberg manifold. Note the prominent avoided crossing near 16 kV/cm, as well as other avoided crossings in the inter- n mixing region.

$n=10$ Rydberg manifold, as apparent in Fig. 4. The driving frequency of 393.8 GHz is nearly resonant with the energy gap at the avoided crossing at 16 kV/cm. As will be shown below, there are no sharp intramanifold resonances at low fields at this frequency, in contrast to the He example discussed above. For simplicity, we have chosen a relatively low-lying Rydberg state; the number of quasienergy states is small enough to easily correlate the transition probabilities with the quasienergy spectra, as well as with the dc field Stark map.

Figure 5 displays the quasienergy spectrum and the $11s$ state survival probability obtained using Shirley's method. The zero-field basis consisted of the $\{n=11, l=0, 1\}$ and $\{n=10, l \geq 2\}$ states. Fifty-one harmonics of the field were used to obtain a periodic center spectrum. The zero-field basis is insufficient to produce an accurate dc Stark map, and the resonant structures apparent in Fig. 5(b) are artificial, owing to inadequate convergence of the atomic basis.

The results of an analogous calculation using the discrete-time picture are shown in Fig. 6. Again, only those adiabatic states corresponding to $\{n=11, l=0, 1\}$ and $\{n=10, l \geq 2\}$ at zero field were used in the basis. With $K=25$, the dimensions of the Floquet matrices used for Figs. 5 and 6 are identical. Note that the low-field resonances do not appear in the discrete-time result of Fig. 6(b). Furthermore, a resonant feature has appeared at the position of the avoided crossing on the dc Stark map (Fig. 4). The feature appears nearly discontinuous, but actually has a finite width related to the avoided crossing of the corresponding quasienergies in Fig. 6(a).

The correspondence between avoided crossings in the dc Stark map and in the quasienergy spectrum is now quite remarkable at this driving frequency. The $11s$ state at zero field occurs at an energy of -1112.2 cm^{-1} in Fig. 6(a). Directly below this level is the $10d$ state, and below $10d$ lies the $11p$ energy. Note how the p and d levels interact strongly near 5 kV/cm and that both of these states drive a state from the degenerate manifold near 6 V/cm. The $11s$ state remains largely uncoupled from all of the other states until the field amplitude reaches the crossing near 16 kV/cm.

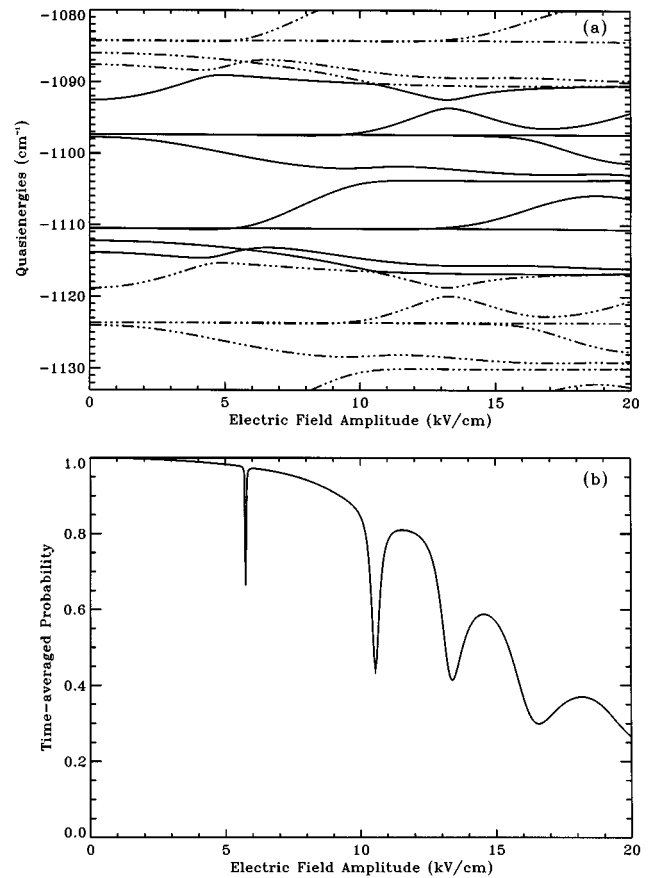


FIG. 5. (a) Map of quasienergy levels as a function of field amplitude for Na atoms in a 393.8-GHz oscillatory, electric field. Results were obtained using Shirley's Floquet Hamiltonian with ten zero-field states in the basis. (b) Resultant survival probability of the $11s$ state as a function of field amplitude.

Note that the departure from unitarity of the discrete-time calculation approaches 20% at the largest fields studied. This is to be expected since Na is known to ionize at fields large enough to induce inter- n transitions [9], implying that no truncated basis of discrete states will completely suffice to describe the dynamics at these fields. However, the resonance feature described above is remarkably insensitive to the number of adiabatic states included in the basis. Figure 7 displays an equivalent discrete-time calculation including two complete manifolds of Rydberg states [$\{n=11, l=0-10\}$, $\{n=10, l \geq 2\}$, and $\{n=12, l=0, 1\}$]. The resonance associated with the $11s \rightarrow n=10$ avoided crossing is still apparent, but its shape is modified by similar resonant structures associated with the $n=10 \rightarrow n=11$ nonadiabatic transitions. Note that the degree of nonunitarity has not changed substantially by including the second manifold. (Preliminary calculations suggest that including transitions to the $n=9$ manifold will substantially decrease the degree of nonunitarity.)

Our results for the intermanifold transitions are shown in Fig. 8. The solid curve indicates the total transition probability to states above the $11p$ state [that is, $\{n=11, l \geq 2\}$ and $\{n=12, l=0, 1\}$]. The manifold states of high angular momentum are dominant, with the $12s$ (dashed) and $12p$ (dot-dashed) states largely unpopulated. The rise of the

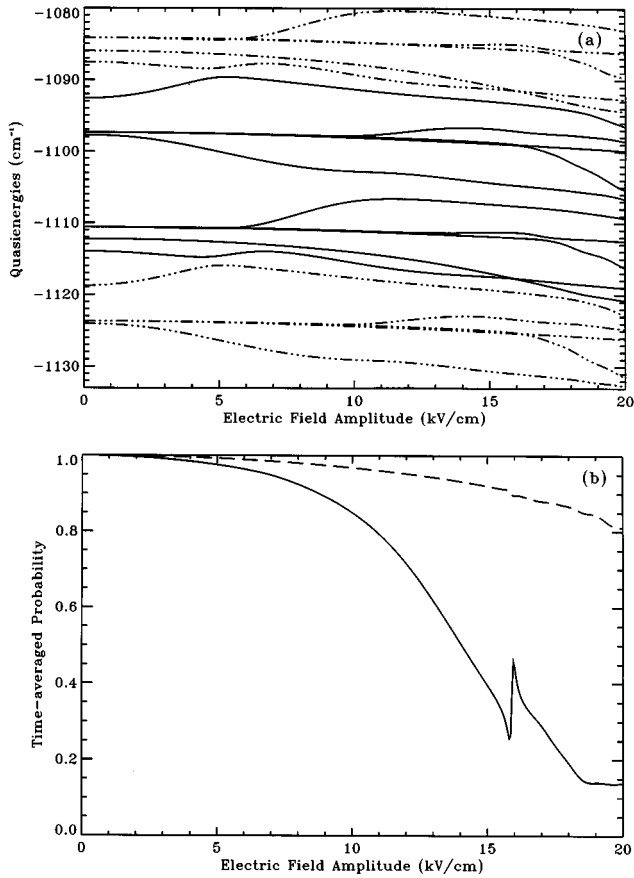


FIG. 6. Same as Fig. 5, but calculated using the discrete-time-transformed Floquet Hamiltonian with ten adiabatic states. (a) Quasienergy spectrum. (b) Survival probability of the $11s$ state. The dashed line is the degree of unitarity of the calculation.

$n \rightarrow n+1$ excitation probability in the vicinity of the adiabatic crossings of the dc Stark map supports the view [9] that this transition is the first and rate-limiting step required for the subsequent excitation and ionization of the atom. How-

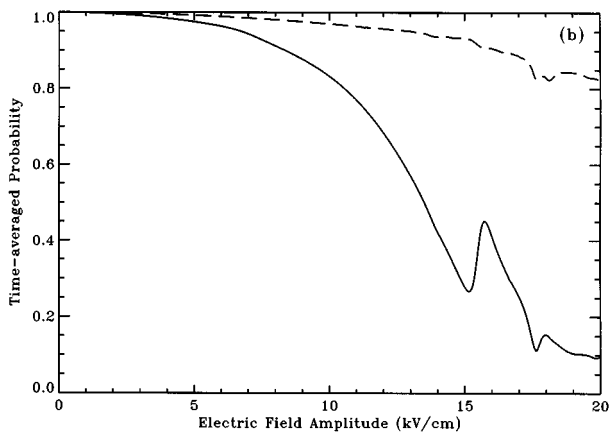


FIG. 7. Survival probability of the $11s$ state as a function of the field amplitude based on 21 adiabatic states corresponding to the $n=10$ and $n=11$ Rydberg manifolds. Note how the resonance near 16 kV/cm has broadened in comparison to Fig. 5(b). The degree of unitarity (dashed line) has not changed appreciably from the ten-state calculation, Fig. 5(b).

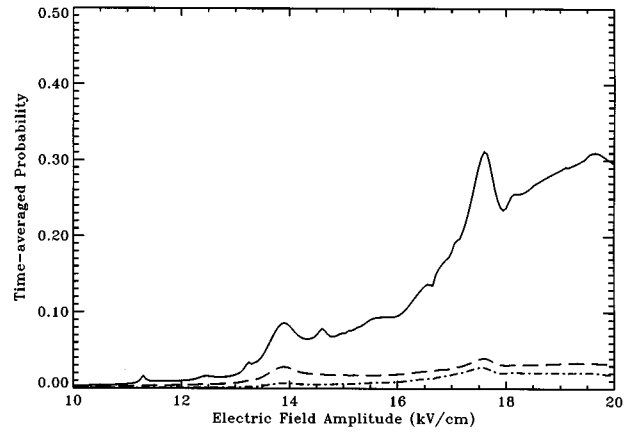


FIG. 8. Transition probability from the $11s$ state to states of the upper manifold $\{n=11, l \geq 2\}$ and $\{n=12, l=0,1\}$. Dashed-curve, $12s$ final state; dot-dashed curve, $12p$ final state.

ever, the intermanifold excitation probability occurs over a fairly broad range of field amplitudes, much broader than the intramanifold Landau-Zener resonance, supporting the conclusion in [11].

VII. SUMMARY

In conclusion, we have provided an alternative formulation of the Floquet approach to the multiphoton, microwave spectroscopy of Rydberg states. A unitary transformation of the truncated Floquet Hamiltonian is all that is required to permit the use of time-dependent basis states in Floquet calculations. Calculations within the adiabatic basis make full use of PT symmetry and require about twice the CPU time of more standard calculations. The calculations are, accordingly, still quite elementary and require only an accurate code for calculating Rydberg states in dc fields. The resulting transition probabilities are considerably more accurate than standard methods in the intermediate-field region.

We have also provided evidence for a resonance feature of multiphoton microwave transitions attributed to Landau-Zener-type excitations on the dc Stark map. In complex systems, this resonance may be obscured by other, sharper resonant features associated primarily with intramanifold transitions. However, the resonance should be observable in atomic Na, provided that the driving frequency is close to the Landau-Zener level splitting.

More fundamentally, we have simply illustrated that Floquet analysis, in its standard form, is essentially equivalent to a discretization in time of Schrödinger's equation over a half cycle of the driving field. Further applications of this technique are in progress.

ACKNOWLEDGMENTS

We are indebted to David A. Harmin, Francis Robicheaux, Peter Koch, and Thomas Gallagher for helpful discussions during the course of this work. We also thank Ugo Fano for a careful reading of the manuscript. This research is supported by the Division of Chemical Sciences, Offices of Basic Energy Sciences, Office of Energy Research, U.S. Department of Energy.

- [1] J. H. Shirley, *Phys. Rev.* **138**, B979 (1965).
- [2] See, for example, E. L. Ince, *Ordinary Differential Equations* (Dover, New York, 1956), Chap. 15, or other works on differential equations.
- [3] See also S. H. Autler and C. H. Townes, *Phys. Rev.* **100**, 703 (1955).
- [4] For a review see Shih-I Chu, *Adv. At. Mol. Phys.* **21**, 197 (1985).
- [5] M. Cavagnero, *Phys. Rev. A* **52**, 2865 (1995).
- [6] J. C. Light, I. P. Hamilton, and J. V. Lill, *J. Chem. Phys.* **82**, 1400 (1985).
- [7] S. E. Choi and J. C. Light, *J. Chem. Phys.* **90**, 2593 (1989).
- [8] J. T. Muckerman, *Chem. Phys. Lett.* **173**, 200 (1990).
- [9] T. F. Gallagher, *Rydberg Atoms* (Cambridge University Press, Cambridge, 1994), Chap. 10.
- [10] A. Maquet, Shih-I Chu, and W. P. Reinhardt, *Phys. Rev. A* **27**, 2946 (1983).
- [11] W. van de Water, K. A. H. van Leeuwen, S. Yoakum, E. J. Galvez, L. Moorman, B. E. Sauer, and P. M. Koch, *Phys. Rev. A* **42**, 572 (1990).
- [12] See, for example, K. R. Symon, *Mechanics*, 3rd ed. (Addison-Wesley, Reading, MA, 1971), Sec. 8.4.
- [13] M. L. Zimmerman, M. G. Littman, M. M. Kash, and D. Kleppner, *Phys. Rev. A* **20**, 2251 (1979).
- [14] S. Yoakum, Ph.D. thesis, State University of New York at Stony Brook, 1992.
- [15] S. Yoakum, W. van de Water, L. Moorman, T. van Leeuwen, and P. Koch, *Phys. Rev. A* **43**, 4065 (1991).